www.czasopisma.pan.pl PAN POLSKA AKADEMIA NAUK www.journals.pan.pl

A R C H I V E S O F M E T A L L U R G Y A N D M A T E R I A L S

Volume 60 2015 Issue 3

DOI: 10.1515/amm-2015-0324

R. DYJA*, E. GAWROŃSKA*,#, N. SCZYGIOL*

THE EFFECT OF MECHANICAL INTERACTIONS BETWEEN THE CASTING AND THE MOLD ON THE CONDITIONS OF HEAT DISSIPATION: A NUMERICAL MODEL

WPŁYW ODDZIAŁYWAŃ MECHANICZNYCH MIĘDZY ODLEWEM A FORMĄ ODLEWNICZĄ NA WARUNKI ODDAWANIA CIEPŁA: MODEL NUMERYCZNY

We present a description of the effects of thermal interactions, which take into account formation of a shrinkage gap, that affect the level of stresses in a system casting – mold. Calculations were carried out in our own computer program which is an implementation of the finite element method used to solve the equations describing a thermo-elastic-plastic model of material and the heat conduction, including solidification. In the computing algorithm we use our own criteria for mechanical interaction between the casting and mold domains. Our model of mechanical interactions between the casting and the mold allows efficient modeling of stresses occurring in the casting and an impact of development of the shrinkage gap on cooling course.

Keywords: shrinkage gap, solidification process, heat dissipation, thermo-elastic-plastic model, thermal resistance

W artykule przedstawiamy opis oddziaływań cieplnych, uwzględniający tworzącą się szczelinę skurczową, które wpływają na poziom naprężeń w układzie odlew – forma odlewnicza. Obliczenia przeprowadzono we własnym programie komputerowym będącym implementacją metody elementów skończonych użytej do rozwiązania równań opisujących termosprężysto–plastyczny model materiału oraz przewodzenia ciepła z uwzględnieniem krzepnięcia. W algorytmie obliczeniowym wykorzystujemy własne kryteria wzajemnego oddziaływania mechanicznego obszarów odlewu i formy odlewniczej. Opracowany model oddziaływań mechanicznych między odlewem a formą odlewniczą pozwala na efektywne modelowanie naprężeń powstających w odlewie oraz wpływ rozwoju szczeliny skurczowej na przebieg stygnięcia.

1. Introduction

During the solidification, and then cooling, generally a shrinkage gap or mechanical interaction (grip or slip) can occur between the casting and the mold. The character of interaction is decided by the shape of casting. Both these phenomena occur in most real castings. Shrinkage gap, and specifically its width, determines the heat flow between cast and mold, while the mechanical interactions lead to increased stress in the solidified layer [11]. If these stresses exceed the limit value, they can damage the solidified layer and, consequently, cause the emergence of casting defects. In most numerical simulations the mechanical interactions are not considered. In the case of shaped casting solidification modeling, only factors affecting the thermal conductivity of the shrinkage gap are taken into account in the heat calculation [2, 12, 13, 14].

The casting structure properties are determined by the push of solute from the growing solid phase, together with the thermal processes and the liquid phase movement. The increasing solid phase forms a skeleton that has the ability to transfer the mechanical loads. Depending on the type of structure, the ability to transfer mechanical loads emerges for different values of the local solid phase fraction.

Diverse temperature gradients together with the resistance put up by the mold are the cause of stress in the solidifying castings, mechanical interaction and shrinkage gap occurrence [1, 4]. The cooling casting shrinkage is the sum of shrinkage caused by temperature and phase change. The stresses are transferred by the solid phase – in the casting domains completely solidified or by the inter-granular layers - in the not fully solidified casting domains. The deformations caused by the mechanical reactions of solidifying casting and mold are small and therefore the friction forces can be neglected in mathematical description of the problem. The shrinkage gap has the greatest impact on the heat exchange between the casting and the mold. Its inclusion in the numerical model of solidification, however, requires carrying out simulations including both the solidification and the stresses formation [8].

Thermo-mechanics of solidification is a very complex field, which consists a lot of phenomena, usually coupled [7].

* CZESTOCHOWA UNIVERSITY OF TECHNOLOGY, INSTITUTE OF COMPUTER AND INFORMATION SCIENCES, FACULTY OF MECHANICAL ENGINEERING AND COMPUTER SCIENCE, 69 DABROWSKIEGO STR., 42-201 CZESTOCHOWA, POLAND

Corresponding authors: elzbieta.gawronska@icis.pcz.pl

Numerical model of the thermo-mechanical phenomena in the solidifying casting and the mold should take into account the coupling of these phenomena. However, the coupling does not significantly affect the determination of values describing the process, so computer simulations of the thermo-mechanical phenomena are carried out as unconjugated. It is possible, however, "simultaneously" to carry out computer simulations of several thermo-mechanical phenomena, coupled with each other through the boundary conditions. In casting process these couplings are very important. At each time step, the computer simulations are carried out alternately. The results of solidification simulation are obtained first and then, in the same time step, they are used to simulate the thermo-mechanical effects. Computer simulations of the thermo-mechanical phenomena coupled through the boundary conditions are very time consuming and require the use of high performance computers or efficient methods employing the physical properties diversity of the modeled domains [5, 6].

This paper takes into account only selected parts of the thermo-mechanical modeling occurring during the production of castings, namely the determination of the thermo-elastic-plastic conditions in the solidifying casting and the mold, as well as mechanical interactions between them. Numerical simulations carried out in presented work, relate to an aluminum - copper alloy, which was selected for two main reasons: first - these alloys are increasingly used in the manufacture of castings, second - the results of tests carried out on this alloy can be easily found in the literature. Research conducted on two-component alloys can serve as a model to test the proper operation of computer programs.

Based on the assumption of small deformations, the thermo-elastic-plastic material model was used. For this material, it was assumed the Huber-Mises-Hencky's yield condition (HMH condition), the isotropic strengthening and associated plastic flow law. The thermo-elastic-plastic states were determined with the use of an explicit integration scheme. In the numerical modeling of contact, the criteria for mechanical interaction between the domains were presented. We specified a geometric and load criterion, in which directions of nodal forces determine the overlapping or separating domains. We assumed that there is no friction between boundaries of the interacting domains. With this assumption, we introduced a slip condition which modify the global system of equations obtained by the use of the finite element method. We performed the numerical simulations of the stresses formation and mechanical interactions between the two-component alloy (Al - 2% Cu) casting and the metal mold. For the considered system (solidifying casting - mold) we assumed the plane stress state. We showed the results of simulation as effective stress distributions in selected casting nodes, shrinkage gap development and the finite element mesh displacements of the casting and mold domains.

We focused on interactions between the casting and the mold. Creep and relaxation phenomena are very interesting, but they don't affect the geometrical criterion of interactions between the casting and mold domains, which is the main theme of paper. However, we decided to take into account plastic strains and temperature influence on the Young's modulus and yield strength in order to obtain more realistic results of stress levels. Unloading phase in the stress-strain paths will occur in the mold during its cooling. Impact of the multiple loading-unloading phases on physical properties is very interesting issue. However, as in the case of creep and relaxation phenomena, it should not affect the geometrical criterion of the casting and mold interaction.

2. Stress modeling during solidification

The material model is described by the relationships between stresses and deformations, obtained by experiment, and the relationships between deformations and displacements obtained from geometrical considerations. Both the material of solidifying/cooling casting and the material of mold can be subject to the thermal, elastic and plastic deformations. There is isotropic strengthening during the plastic deformation of these materials. Since the deformations that occur in the casting and the mold are small, the total deformation can be expressed as the following sum:

$$\boldsymbol{\varepsilon} = \boldsymbol{\varepsilon}^{el} + \boldsymbol{\varepsilon}^{th} + \boldsymbol{\varepsilon}^{pl} \tag{1}$$

where $\boldsymbol{\varepsilon}^{el}$ is elastic deformation vector, $\boldsymbol{\varepsilon}^{th}$ is thermal deformation vector and $\boldsymbol{\varepsilon}^{pl}$ is plastic deformation vector.

The transition of material from an elastic state to a plastic state is only possible if the stress satisfies a function known as an yield condition. For metals and their alloys the HMH condition is used, which states that the material is plasticized when the deviatoric deformation energy reaches a certain, characteristic for given material, limit value.

Due to the incremental nature of the plastic flow law, the elastic-plastic problems need to be solved through the small load increments (incremental methods) [3, 9]. For each step (load increment) stresses and strains increments are calculated, which are then added to the previously calculated stresses and strains. Using the finite element method to determine the thermo-elastic-plastic states, the displacement increase in a single step, corresponding to the load increment, is obtained from the solution of the following equation system:

$$\mathbf{K}\Delta\mathbf{u} = \Delta\mathbf{R} \tag{2}$$

where $\mathbf{K}$ is stiffness matrix, $\Delta\mathbf{u}$ is displacement increments vector and is load increments vector.

In our discussion we use an enthalpy formulation of solidification with a full approximation of enthalpy:

$$\mathbf{M}\dot{\mathbf{H}} + \mathbf{K}(T)\mathbf{T} = \mathbf{b}(T) \tag{3}$$

where $\mathbf{H}$ is enthalpy, $\mathbf{M}$ is mass matrix, $\mathbf{b}$ is right-side hand vector, $\mathbf{T}$ is temperature vector, and the indirect solid phase growth model [15, 16]:

$$f_s(T) = \frac{1}{1-nk\alpha}\left(1 - \left(\frac{T_M - T}{T_M - T_L}\right)^{\frac{1-nk\alpha}{k-1}}\right) \tag{4}$$

where n is grain aspect coefficient, k is partition solute coefficient, α is the Brody-Flemings coefficient, T_M is pure metal solidification temperature and T_L is liquidus temperature.

At the stage of solidification, stresses occur when the coherent solid phase skeleton forms. Therefore, the solidification degree of particular casting domains determines

the stress formation. In the numerical modeling of stresses in casting, we should therefore adopt a certain limiting value of the solid phase fraction in a finite element (or node), from which the process of stress formation begins. It can be assumed that the solid phase skeleton is coherent, if the solid phase fraction is greater than a predefined threshold.

In order to calculate the stress is therefore necessary to know the temporal temperature and solid phase fraction fields. In this work it is assumed that in the solidification and stress numerical models do not occur coupling parts. The numerical solidification and stress calculations can be coupled via the boundary conditions. Coupling by boundary conditions results in solidification and stress calculations conducted alternately for each time step. This approach allows taking into account the shrinkage gap formation (increasing the heat exchange resistance between the casting and the mold) in the heat calculation, which in turn can change the level of stresses in the analyzed system of casting - mold.

3. Numerical modeling of contact

Mechanical interaction between the casting and the mold are the result of resistance, which is caused by the rigid parts of shrinking casting and the mold. Because the casting and mold domains in the finite elements mesh are separated from each other, therefore the stresses, forming in both domains, are not carrying through their boundaries. The finite element mesh is deformed independently, unless the casting and the mold are coupled by a corresponding boundary condition (continuity or slip). Binding domains by continuity conditions takes place until the formation of a coherent solid phase layer able to carry stresses. When the coherent solid phase layer interacts mechanically with the mold, the slip condition bind domains. Each of these conditions must take into account the both possibilities: the mechanical interaction or the separation of domains. If the shrinkage gap has formed on a part of boundary, we assumed that two domains for this fragment of the boundary are not bind. The introduction of the so-defined boundary conditions occurs before performing the calculations for the given step of load.

3.1 Mechanical interaction domains criteria

During the numerical modeling of mechanical interactions between the mold and the casting, in which coherent solid phase layer was formed, we must check whether parts of the domains overlap or move away from each other. This checking is done using a geometric criterion (Fig. 1).

If in the previous calculation step, the boundaries of domains were in contact, then their further impact or their moving is verified by a criterion involving a determination of force components at the nodes lying on the separated boundaries. The force at nodes is calculated for one of the domains as follows:

$$\mathbf{F} = \sum_{1}^{eb} \int_{\Omega^e} \mathbf{B}^T \boldsymbol{\sigma} \, d\Omega \tag{5}$$

where **F** is nodal force vector (reaction), **B** is matrix containing shape functions derivatives, eb is number of elements in domain connected with node on boundary and $\boldsymbol{\sigma}$ is designated stress in the current iteration. On the basis of the nodal force components, the resultant force is calculated and its direction is checked. If it is directed inward the concerned domain, it means that these domains mechanically interact (Fig. 2). Otherwise, the shrinkage gap is formed.

After finding the mechanical interactions on the part of boundary, the system of equations should be modified and re-calculation performed. The system of equations modification is carried out using the contact condition (slip). In the case of separating domains, the system of equations modification is not carried out.

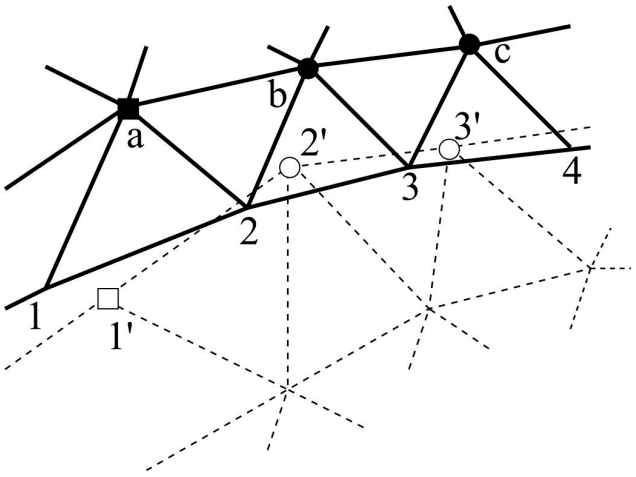

Fig. 1. Identification of nodes in overlapping domains

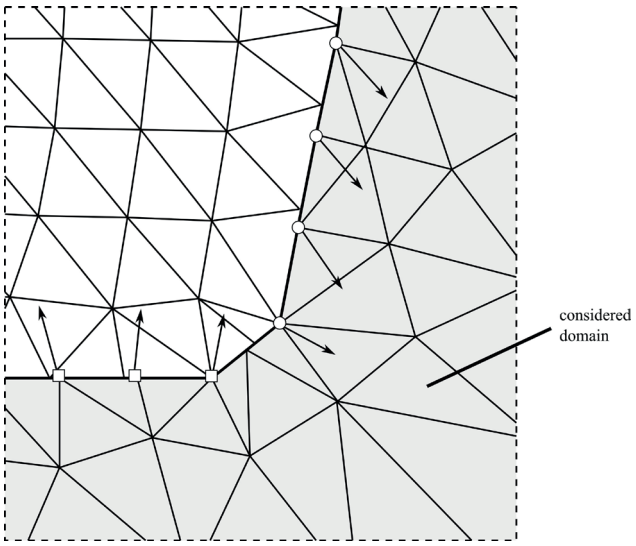

Fig. 2. Identification of nodes in separating and overlapping areas (□ shrinking gap, ○ mechanical interaction)

3.2 Slip condition

In the case of mechanical interaction between domains, it is assumed they slide without friction. This is achieved by forcing equality displacement for a pair of nodes in normal direction to movement direction (Fig. 3). As a result, both nodes are still on a line parallel to their previous position, but do not need to occupy the same positions.

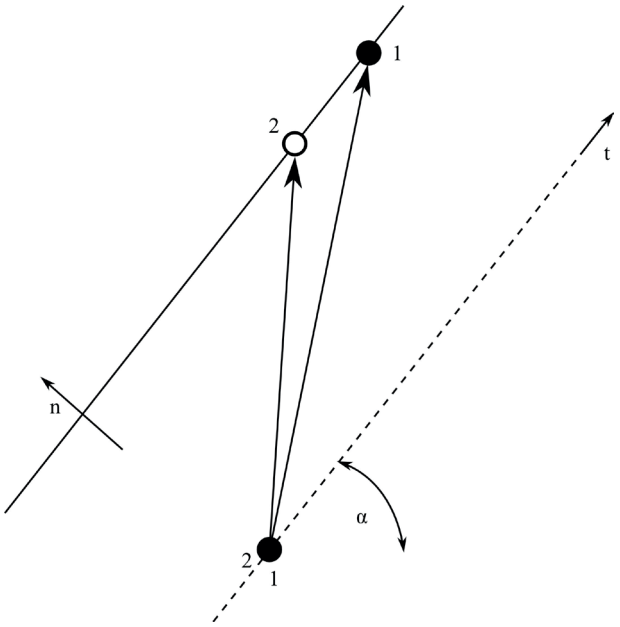

Fig. 3. Pair of nodes equality displacement condition normal to their movement direction

The pair of nodes equality displacement condition normal to their movement direction, in a generalized form, can be described as follows:

$$q_i + aq_{i+1} + bq_j + cq_{j+1} = d \tag{6}$$

where q is generalized displacement of nodes, i, j are subscripts representing the numbers of nodes displacements in the global system of equations, and coefficients a,b,c i d are responsible for the transformation during projection of displacements on the normal direction.

Introduction of the slip condition to the system of equations is associated with corresponding modifications in both the matrix of coefficients and the right-side hand vector.

4. Computation algorithm

First, we assume the elastic behavior of casting material. This assumption holds true in successive time steps. If at any time step in any finite element the transition from elastic state to elastic-plastic one follows, it means that the calculated increments of deformation are incorrect. They should be corrected by the simultaneous specification of the plastic deformation increment. This is an iterative process. It is also used for pre-plasticized elements. To calculate the plastic strain increments we used an explicit scheme and the method of initial stiffness (i.e. the constant stiffness in one step of load) [10].

The calculation algorithm presented below only applies to the determination of thermo-elastic-plastic states and does not take into account the mechanical interactions occurring between the casting and the mold. Subsequent stages of the algorithm for one time step, i.e. a temperature increment, are as follows:

1. For all finite elements:
   a. build and solve the system of equations Eq. (2) to calculate the displacement increment
2. For each element, with the solid phase fraction above the limit value:
   a. calculate the strain increment $\Delta\varepsilon = \mathbf{B}\Delta u$ and the stress increment $\Delta\boldsymbol{\sigma}^{el}$,
   b. check the plastic deformation criterion; element becomes elastic-plastic when its effective stress exceeds plastic stress value,
   c. if element is in the elastic state proceed to point 7,
   d. if element is in the elastic-plastic state, calculate the total deformation, total stress and

$$\Delta\boldsymbol{\varepsilon}^{ep} = \Delta\boldsymbol{\varepsilon}^{el} + \Delta\boldsymbol{\varepsilon}^{pl} = \Delta\boldsymbol{\varepsilon} - \Delta\boldsymbol{\varepsilon}^{th} \tag{7}$$

   if at the previous time step element was in the elastic state, modify these values according to the point of plastic deformation,
   e. calculate the plasticity multiplier increment and the plastic deformation increment
3. Correct the strain increment. For this purpose, construct the load vector:

$$\delta\mathbf{R} = \sum_{1}^{ne} \int_{\Omega^e} \mathbf{B}^T\mathbf{C}\mathbf{B}\delta\varepsilon^{pl}\, d\Omega \tag{8}$$

   where ne is number of finite elements in mesh and

$$\delta\boldsymbol{\varepsilon}^{pl} = \boldsymbol{\varepsilon}_i^{pl} - \Delta\boldsymbol{\varepsilon}_{i-1}^{pl} \tag{9}$$

   is the difference of deformation increments in two successive iteration steps (i). In the first iteration adopt $\delta\boldsymbol{\varepsilon}^{pl} = \Delta\boldsymbol{\varepsilon}^{pl}$
4. Solve the system of equations:

$$\mathbf{K}\delta\mathbf{u} = \delta\mathbf{R} \tag{10}$$

   For each element:
   a. calculate the correction of deformation increment $\delta\varepsilon = \mathbf{B}\delta u$ and upgrade the strain increment

$$\Delta\boldsymbol{\varepsilon}_{i+1} = \Delta\boldsymbol{\varepsilon}_i + \delta\boldsymbol{\varepsilon} \tag{11}$$

   calculate the plasticity multiplier increment, the plastic deformation increment and

$$\delta\boldsymbol{\varepsilon}_{i+1}^{pl} = \Delta\boldsymbol{\varepsilon}_{i+1}^{pl} - \Delta\boldsymbol{\varepsilon}_i^{pl} \tag{12}$$

   check the convergence condition

$$\left|\delta\bar{\boldsymbol{\varepsilon}}_{i+1}^{pl} - \delta\bar{\boldsymbol{\varepsilon}}_i^{pl}\right| \le TOL \tag{13}$$

   where TOL is predetermined calculations accuracy.
5. If the convergence condition is satisfied for all elements, go to point 7, otherwise go to point 3
6. For each element:
   a. if element is in the elastic-plastic state calculate the stress increment,
   b. update the deformation and stress by adding increments to their values from the previous time step.

In order to enforce the contact condition, the modification of equations system should be carried out before its solution. The algorithm realizing the introduction of the slip condition Eq. (6) to the global system of equations is as follows:

1. columns modification:
   a. from column $i+1$ subtract column i multiplied by a,
   b. from column j subtract column i multiplied by b,
   c. from column $j+1$ subtract column i multiplied by c,
   d. from right-side hand vector subtract column i multiplied by d,
2. reset column i,
3. rows modification:
   a. from row $i+1$ subtract row i multiplied by a,
   b. from row j subtract row i multiplied by b,
   c. from row $j+1$ subtract row i multiplied by c,
4. reset row i,
5. in row i insert:
   a. 1 in column i,
   b. a in column $i+1$,
   c. b in column j,
   d. c in column $j+1$,
   e. d in right-side hand vector.

The system of equations modifications Eq. (2) carried out in accordance with the above algorithm, which can be temporarily saved as:

$$\mathbf{Kq} = \mathbf{r} \tag{14}$$

are shown in Fig. 4.

5. Results and discussion

Our implementation was tested with an example presented in Fig. 5, where the dimensions of casting and metal mold are shown. The computational domain of casting was divided into 3921 finite elements, while the mold was divided into 5191 elements. Material of casting was Al - 2%Cu alloy and the mold was made from steel. The material properties used in the solidification simulations are summarized in TABLE 1.

TABLE 1:
Material properties used in solidification simulation

	Liquid	Solid	Mold
ρ, kg/m^3	2498	2824	7500
c, J/kgK	1275	1077	620
λ,W/mK	104	262	40
L, J/kg	390000		
K	0.125		

The heat exchange between the mold and environment was modeled by using the boundary condition of 3. type with the heat exchange coefficient equal to 100 W/m^{2}K on the upper and side walls and 50 W/m^{2}K on the bottom wall. The boundary condition of 4. type (heat exchange between two domains with boundary layer) was used to model the heat exchange between the mold and casting. The heat exchange coefficient of boundary layer was equal to 1000 W/m2K. The time step was equal to 0.05 s.

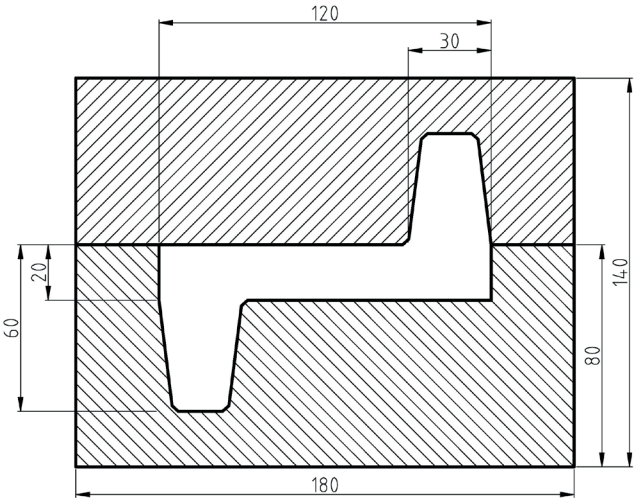

Fig. 5. View of the mold and the casting with dimensions

$$\begin{bmatrix}
k_{1,1} & \cdots & 0 & k_{1,i+1}-ak_{1,i} & \cdots & k_{1,j}-bk1,i & k_{1,j+1}-ck_{1,i} & \cdots & k_{1,n} \\
\cdots & \cdots & \cdots & \cdots & \cdots & \cdots & \cdots & \cdots & \cdots \\
0 & \cdots & 1 & a & \cdots & b & c & \cdots & 0 \\
k_{i+1,1} - ak_{i,1} & \cdots & 0 & k_{i+1,i+1}-ak_{i+1,i} - ak_{i,i+1}+a^2k_{i,i} & \cdots & k_{i+1,j}-bk_{i+1,i} - ak_{i,j}+abk_{i,i} & k_{i+1,j+1}-ck_{i+1,i} - ak_{i,j+1}+ack_{i,i} & \cdots & k_{i+1,n} - ak_{i,n} \\
\cdots & \cdots & \cdots & \cdots & \cdots & \cdots & \cdots & \cdots & \cdots \\
k_{j,1} - bk_{i,1} & \cdots & 0 & k_{j,i+1}-ak_{j,i} - bk_{i,i+1}+abk_{i,i} & \cdots & k_{j,j}-bk_{j,i} - bk_{i,j}+b^2k_{i,i} & k_{j,j+1}-ck_{j,i} - bk_{i,j+1}+bck_{i,i} & \cdots & k_{j,n} - bk_{i,n} \\
k_{j+1,1} - ck_{i,1} & \cdots & 0 & k_{j+1,i+1}-ak_{j+1,i} - ck_{i,i+1}+ack_{i,i} & \cdots & k_{j+1,j}-bk_{j+1,i} - ck_{i,j}+bck_{i,i} & k_{j+1,j+1}-ck_{j+1,i} - ck_{i,j+1}+c^2k_{i,i} & \cdots & k_{j+1,n} - ck_{i,n} \\
\cdots & \cdots & \cdots & \cdots & \cdots & \cdots & \cdots & \cdots & \cdots \\
k_{n,1} & \cdots & 0 & k_{n,i+1}-ak_{n,i} & \cdots & k_{n,j}-bk_{n,i} & k_{n,j+1}-ck_{n,i} & \cdots & k_{n,n}
\end{bmatrix}
\cdot
\begin{pmatrix} q_1 \\ \cdots \\ q_i \\ q_{i+1} \\ \cdots \\ q_j \\ q_{j+1} \\ \cdots \\ q_n \end{pmatrix}
=
\begin{pmatrix} r_1-dk_{1,i} \\ \cdots \\ d \\ r_{i+1}-dk_{i+1,i} - ar_i+adk_{i,i} \\ \cdots \\ r_j-dk_{j,i} - br_i+bdk_{i,i} \\ r_{j+1}-dk_{j+1,i} - cr_i+cdk_{i,i} \\ \cdots \\ r_n-dk_{n,i} \end{pmatrix}$$

Fig. 4. Global system of equations after modification

The material properties used in the thermo-elastic-plastic model for casting material are:

The Young's modulus of casting material:

$$E(T) = \begin{cases} 2.5 \cdot 10^2 \left(\frac{913 - T}{100}\right)^2 & \text{for } 813 \leqslant T \leqslant 913 \\ 2.5 \cdot 10^2 + 5.3 \cdot 10^2 \frac{813 - T}{60} & \text{for } 753 \leqslant T \leqslant 813 \end{cases} \quad (15)$$

The yield strength of casting material:

$$Re(T) = \begin{cases} 2.2 \left(\frac{913 - T}{100}\right)^3 & \text{for } 813 \leqslant T \leqslant 913 \\ 2.2 + 17.8 \frac{813 - T}{60} & \text{for } 753 \leqslant T \leqslant 813 \end{cases} \quad (16)$$

Below 753 K we used a linear interpolation of the Young's modulus and yield strength assuming that in 300 K these values are equal to: E = 72.5 GPa and Re = 290 MPa. The Poisson's ratio is equal to 0.35, regardless of temperature, and the strain hardening index equals 0.1.

The Young's modulus and yield strength of the mold are calculated in temperature interval from 1573 K to 1773 K from formulas:

$$E(T) = 1.379 \cdot 10^{-3}(T - 273)^2 - 22.56(T - 273) + 31291.22 \quad (17)$$

and

$$Re(T) = 0.176 \cdot 10^{-6}(T - 273)^2 - 2.645 \cdot 10^{-2}(T - 273) + 39.85 \quad (18)$$

Below 1573 K we also used a linear interpolation with requirement that properties in 300 K are equal to: E = 207 GPa and Re = 350 MPa. The Poisson's ratio equals to 0.30, regardless of temperature, and the strain hardening index equals to 0.2. We assumed the plastic strains in mold material, because the mold is heated by the casting to temperatures where the yield strength is much lower. Moreover, while the mold is heated, the casting is cooled and its Young modulus increases. This is why we assumed possibility of the plastic strains in mold.

The coefficients of thermal expansion are equal to $4 \cdot 10^{-5}$ 1/K for casting and $1.4 \cdot 10^{-5}$ 1/K for mold.

We assumed the plane stress condition in our calculations. The stress calculations were started in areas where the solid fraction was at least equal to 0.4. All nodes on the bottom side of the mold were fixed in y direction. Additionally one of nodes (in the left corner) was fixed in x direction.

We conducted two versions of calculations:

A – this version assumes no coupling between the solidification and stresses analysis,

B – this version assumes coupling between the solidification and stresses analysis by using the boundary conditions.

These two versions made it possible to investigate influence of the shrinkage gap formation on the solidification process. To express the influence of gap width on the heat exchange coefficient we use following formula:

$$\kappa = \frac{1}{\frac{\delta_p}{\lambda_p} + \frac{\delta_g}{\lambda_g}} \quad (19)$$

where δ is layer width, λ is conductivity and subscript p denotes coating layer, while g denotes gas layer (arisen from nonzero shrinkage gap width).

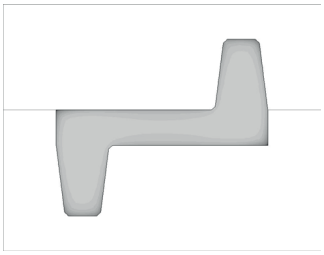

Fig. 6. Cooling speed distribution inside of the casting. Maximum value (58 K/s) is marked in light gray, while minimum value (3K/s) is marked in black

Both versions give very similar results for cooling speed. The maximum obtained cooling speed was equal to 58 K/s and occurred in the corners of casting. Large areas of the casting solidified with much slower velocity of 3 K/s.

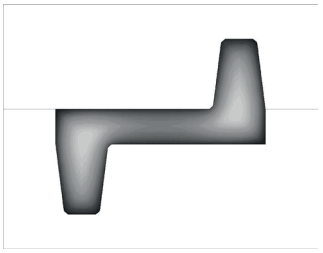

Fig. 7. Distribution of temperature in which solidification is completed. Maximum value (877 K) is marked in light gray, while minimum value (823K) is marked in black

The same situation occurs for temperature in which solidification is completed. Both versions give almost identical results, which are shown in Fig. 7. In the investigated example, temperature in which solidification is completed was between 877 K and 823 K.

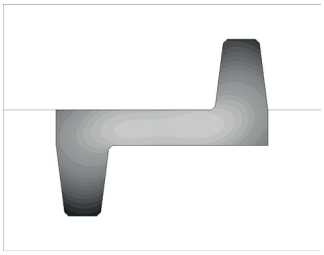

Fig. 8. Temperature field in the casting after 60 s (case A). Maximum value (883 K) is marked in light gray, while minimum value (850 K) is marked in black

Fig. 9. Temperature field in the mold after 60 s (case A). Maximum value (761 K) is marked in light gray, while minimum value (540 K) is marked in black

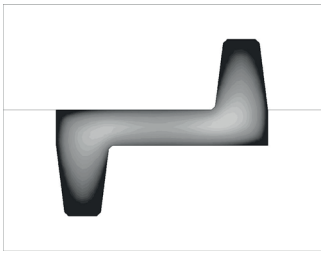

Fig. 10. Solid fraction distribution in the casting after 60 s (case A). Maximum value (1.00) is marked in black, while minimum value (0.93) is marked in light gray

The temperature field in the casting and the mold after 60 s of simulation for version A are shown in Fig. 8 and Fig. 9, accordingly. As we can see from Fig. 9 the casting is not fully solidified, however all parts are solid enough to carry stresses. The effective stresses for version A are shown in Fig. 11 for casting and in Fig. 12 for mold.

Fig. 11. Effective stress distribution in the casting after 60 s (case A). Maximum value (0.27 MPa) is marked in light gray, while minimum value (350 Pa) is marked in black

Fig. 12. Effective stress distribution in the mold after 60 s (case A). Maximum value (217 MPa) is marked in light gray, while minimum value (350 Pa) is marked in black

The stresses are caused mainly by the resistance which the mold raises to the shrinking material. This causes bending upper and lower parts of the casting. The left part of casting is bend so much that hits upper part of the mold. A view of deformed mesh (with deformation amplification of 20x) is shown in Fig. 13, while Fig. 14 shows domains of the plastic deformation.

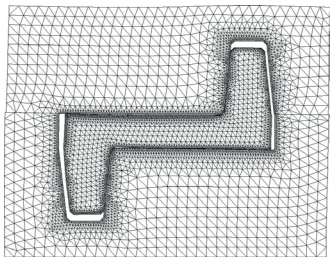

Fig. 13. Mesh deformation (case A). The deformation was amplified by factor 20 in order to visualize the shrinking gap

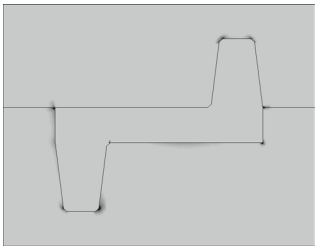

Fig. 14. Plastic strain after 60 s (case A). Places, where the plastic strains occur are black

Figs. 15-21 show results for case B. From these pictures we can see the impact of coupling on the solidification temperature. In this version the casting solidified slower than in case A, especially in the bottom part. Because of different temperature fields, some differences in the stress fields can also be observed.

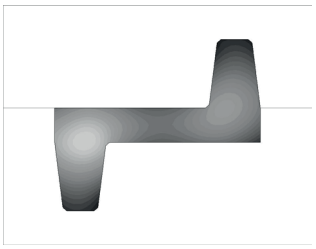

Fig. 15. Temperature field in the casting after 60 s (case B). Maximum value (901 K) is marked in light gray, while minimum value (876 K) is marked in black

Fig. 16. Temperature field in the mold after 60 s (case B). Maximum value (759 K) is marked in light gray, while minimum value (533 K) is marked in black

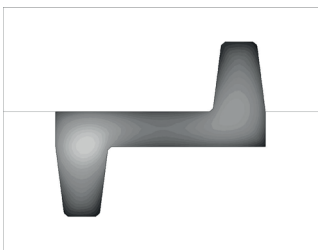

Fig. 17. Solid fraction distribution in the casting after 60 s (case B). Maximum value (1.00) is marked in black, while minimum value (0.93) is marked in light gray

Fig. 18. Effective stress distribution in the casting after 60 s (case B). Maximum value (0.11 MPa) is marked in light gray, while minimum value (95 Pa) is marked in black

Figure 19. Effective stress distribution in the mold after 60 s (case B). Maximum value (191 MPa) is marked in light gray, while minimum value (95 Pa) is marked in black

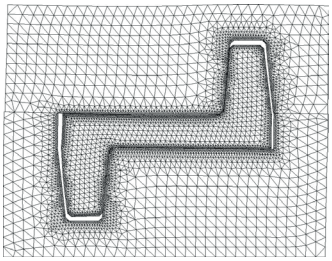

Fig. 20. Mesh deformation (case B). The deformation was amplified by factor 20 in order to visualize the shrinking gap

The more detailed observation of differences can be done with the use of Fig. 22 and Fig. 23, where changes of temperature and stress level are shown as a function of time. These figures were obtained for a point that was located on the boundary between the casting and the mold in the upper right part of casting.

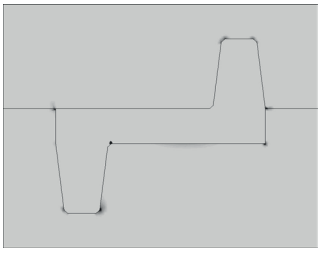

Fig. 21. Plastic strain after 60 s (case B). Places, where the plastic strains occur are black

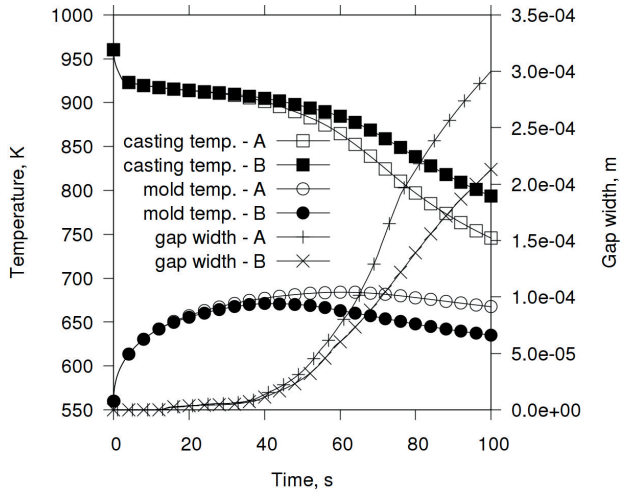

Fig. 22. Cooling curves obtained for a point located on a boundary between the casting and the mold in a top right part of the casting. Additionally, the evolution of gap width is shown. The cooling curves and evolution of gap width are plotted for two cases (A and B)

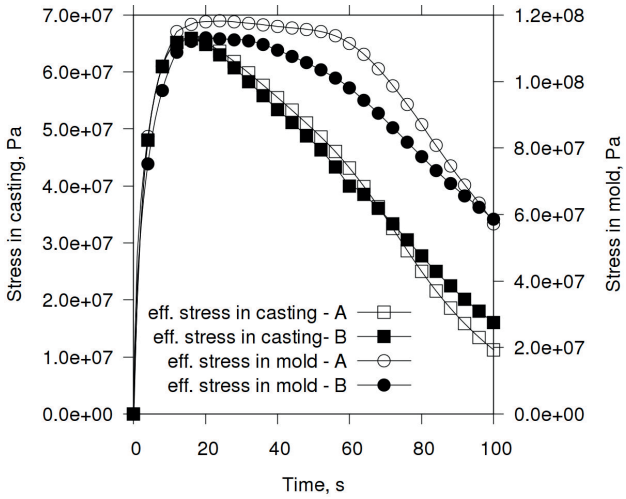

Fig. 23. Evolution of the effective stress in a point located on a boundary between the casting and the mold in a top right part of the casting. The stress evolution curves are plotted for two cases (A and B).

As we can see, after 100 s, the difference in gap width between these two versions is almost 30%, which results in almost 50 K difference in temperature in the region close to boundary. While the level of stresses in the casting was similar for the two cases, the stresses in mold had higher level in case A, especially in time interval 10 – 90 s.

6. Conclusions

We coupled our model of interactions between the casting and the mold with the sophisticated model of thermo-elastic-plastic analysis. The thermal analysis also includes the effects of solid-liquid phase transitions and authors' model of solid phase growth. The test example was based on a complex geometry that allowed testing the slip, grip and separation of two domains. Additionally, we were also able to test the influence of the mechanical interactions between the casting and the mold on the conditions of heat dissipation. Our model shows that this impact should be considered in calculations,

because of observed differences in obtained temperature fields and resulting of these differences in the stress levels.

REFERENCES

[1] S. Bounds, G. Moran, K. Pericleous, M. Cross, T.N.A Croft, Metall Mater Trans B **31**, 3 (2000).
[2] R.J.C. Chaudhary, B. G. Thomas, S. P. Vanka, Metall Mater Trans B **42**, 5 (2011).
[3] M.A. Crisfield, Non-linear Finite Element Analysis of Solids and Structures, Chichester 1991.
[4] L.A. Crivelli, S.R. Idelsohn, Int J Numer Meth Eng, 23 (1986).
[5] E. Gawronska, N. Sczygiol, in: Lect Notes Eng Comp Imecs 2014 Proceedings, IAENG 1256, **2**, Hong Kong (2014).
[6] E. Gawronska, N. Sczygiol, in: IEEE Computer Society SYNASC 2010 Proceedings, T. Ida et al. (Ed.) 588, Timisoara (2010).
[7] J. Guo, M. Samonds, JOM-US **63**, 7 (2011).
[8] J.H. Lee, H.S. Kim, C.W. Won, B. Cantor, Mater Sci Eng A-Struct, 338 (2002).
[9] D.R.J. Owen, E. Hinton, Finite Elements in Plasticity: Theory and Practice, Swansea U.K. 1980.
[10] P. Tauzowski, M. Kleiber, Comput Struct **84** (2006).
[11] B.G. Thomas, Modeling of Casting, Welding and Advanced Solidification Processes VI, T. Piwonka and V. Voller, (Ed.) **6**, Warrendale (1993).
[12] K. Pericleous, M. Cross, P. Chow, C. Bailey, in: Advanced Computational Methods in Heat Transfer III, L.C. Wrobel et al. (Ed), Southampton (1994).
[13] R. Song, G. Dhatt, A. Ben Cheikh, Int J Numer Meth Eng **30** (1990).
[14] H. Wang, G. Djambazov, K.A. Pericleous, R.A. Harding, M. Wickins, Comput Fluids **42**, 1 (2011) .

Received: 20 January 2015.